Journal of Chromatography, 245 (1982) 271–290
Elsevier Scientific Publishing Company, Amsterdam — Printed in The Netherlands

CHROM. 14,954

AFFINITY ELECTROPHORESIS: A THEORETICAL STUDY OF THE EFFECTS OF THE KINETICS OF PROTEIN–LIGAND COMPLEX FORMATION AND DISSOCIATION REACTIONS

VLADIMÍR MATOUŠEK and VÁCLAV HOŘEJŠÍ*
Institute of Molecular Genetics, Czechoslovak Academy of Sciences, Vídeňská 1083, 142 20 Prague 4 (Czechoslovakia)
(First received January 25th, 1982; revised manuscript received March 30th, 1982)

SUMMARY

The kinetics of protein–immobilized ligand interactions during affinity electrophoresis are of great importance for the practical applicability of the method and for the interpretation of the results. Major theoretically predicted effects of the kinetics of (monovalent) protein–immobilized ligand complex formation and decay reactions during affinity electrophoresis are (1) broadening of the protein zone and (2) anomalies at the beginning of the experiment before steady-state conditions are achieved. These phenomena are described quantitatively and experimental consequences are predicted. Experimental procedures for minimizing the adverse effects of slow kinetics are suggested. Affinity electrophoresis can be used safely for the measurement of the apparent dissociation constant of a protein–immobilized ligand complex (from the values of the mobilities of the ligand-binding protein on affinity gels) if the lifetime of the complex is much shorter than the total time of the electrophoretic experiment, *i.e.*, under the conditions normally used approximately $t_{1/2} < 10$ sec. Quantitative analysis of the zone profile of the protein in the affinity gel can yield the kinetic parameters (rate constants) of the protein–immobilized ligand interaction. With very stable complexes (lifetime longer than the duration of the electrophoretic experiment) an alternative technique can be used for measurement of the dissociation constant, *i.e.*, electrophoretic separation of the complex-bound and free protein after establishment of equilibrium. The equations derived are used for prediction of the behaviour of several typical ligand-binding proteins (lectins, antibodies) with characteristic equilibrium and rate constants of the complexation reaction with a ligand.

INTRODUCTION

Affinity electrophoresis (for a review, see ref. 1) can be used both for qualitative purposes (such as the detection and identification of ligand-binding proteins, and the detection of impurities in preparations of such binding proteins) and for quantitative evaluation of the strength of protein–ligand interactions. So far most quantitative applications of affinity electrophoresis (*i.e.*, estimation of the dissociation constants

0021-9673/82/0000–0000/$02.75

of protein–ligand complexes) were based on very simple equations relating the mobility of a protein on an affinity gel to the dissociation constants of the protein–ligand complexes, implicitly assuming a number of simplifying conditions. However, the application of affinity electrophoresis for these quantitative purposes obviously requires the development of a reliable theory of the technique quantitatively describing the effects of various factors that affect the process of protein–ligand complex formation. The effects of a number of factors have been theoretically treated in two previous papers[2,3].

One of the simplifying assumptions used for deriving the relatively simple equations applicable for the evaluation of the dissociation constants of protein–ligand complexes by affinity electrophoresis is that the rates of complex formation and dissociation reactions are very high so that kinetic effects are negligible and the situation in the protein zone moving through the affinity gel is very close to an equilibrium state. However, as affinity electrophoresis is principally a non-equilibrium method, this assumption may not be always valid in practice. Therefore, it was of interest to evaluate the effects of the kinetics of the complex formation reaction on the results obtainable by this technique. The effects of kinetics were partially discussed (in addition to several other factors) in a previous paper[2], but in that study an oversimplified model was used, the effects of kinetics on the distribution of protein molecules (*i.e.*, the width of the band) not being considered.

In this paper we present a fuller description of this problem. The results obtained can be used to predict the kinetic limitations of the technique and to suggest conditions under which the complicating kinetic effects can be eliminated; also, the possibility of measuring rate constants by affinity electrophoresis is demonstrated.

MODEL USED

The characteristic features of the model used are as follows. The medium used as an affinity gel is a highly porous, macroscopically homogeneous gel containing immobilized ligand molecules (concentration c) covalently attached to the gel matrix. The macromolecular gel-forming network has negligible volume so that there are no restrictions to free diffusion of protein molecules within the gel; each point in the gel is accessible to a protein molecule. All immobilized ligands are chemically equivalent and accessible to interaction with the protein; thus, the effective concentration of the immobilized ligand is identical with the total concentration c. The space distribution of ligand molecules is random (statistical). The medium forms a homogeneous block (*e.g.*, a rod in a glass tube) which connects vertically two electrode vessels as usually used in vertical disc electrophoresis apparatus. A single buffer is used throughout the system (*i.e.*, a continuous buffer system is employed). The sample is applied as a very narrow zone at the top of the gel; the molar concentration of the protein (a) in the sample is much lower than c ($a \ll c$). The protein molecule (with diffusion coefficient D) possesses a single ligand-binding site. A potential gradient used is such that the rate of electrophoretic movement of the protein in a control (non-interacting) gel is v. Electroendosmosis of the gel is negligibly low and the temperature is constant.

Mathematical description of the model in the general case

Let the protein molecule be free (uncomplexed at time $t = 0$). After switching

on the electric field it executes Brownian motion for a certain time with drift velocity v in the direction of the line of force until a collision with an immobilized ligand occurs. Now one of two events may occur: either the molecule is intercepted by the ligand with the result that an immobile complex is formed and the molecule comes to rest, or it may bounce off and continue drifting. The latter event may be repeated consecutively several times until the first event recurs. However, as the lifetime of the (immobile) complex is finite, the complex will decay after a certain time and the whole process will start anew. Thus, the complex formation results in retardation of the protein in an affinity gel compared with a control gel. Generally, we wish to find the probability that the protein molecule will occur at a distance s from the start at time $t = T$, *i.e.*, to determine the time-dependent distribution of protein molecules throughout the length of the gel under general conditions. Such a probability distribution should yield the concentration profile of the protein zone at any time (*cf.*, Fig. 2). In order to do so we have to start with some generally plausible assumptions that will enable us to describe mathematically the fate of one randomly selected molecule.

Let ξ_i be the waiting times between consecutive collisions, χ_j the lifetimes of protein complexes that the molecule forms ($i, j = 1, 2, \ldots$) and ω the probability that a collision will be effective, *i.e.*, will result in complex formation. We assume that ξ_i and χ_j are mutually independent exponentially distributed random variables with probability densities

$$\left.\begin{aligned} f_\xi(t) &= \kappa e^{-\kappa t} \\ f_\chi(t) &= \mu e^{-\mu t} \end{aligned}\right\} t > 0 \qquad (1)$$

[It should be noted that the frequently used half-life of the complex is equal to $(\ln 2)/\mu$ but for our purposes the parameter μ is more convenient.] The instances of collision without and with interception divide the interval of observation $[0, T]$ into subintervals of motion and rest as shown in Fig. 1 where the intervals of motion of the molecule are drawn with heavy lines.

The probability ω may be termed the effective cross-section for the complex formation reaction and is assumed to be constant.

It is intuitively clear and can easily be shown by explicit argument that the waiting times τ_j between two consecutive effective collisions are exponentially distributed with the probability density

$$f_{\tau_j}(t) = \omega\kappa e^{-\omega\kappa t} \qquad (2)$$

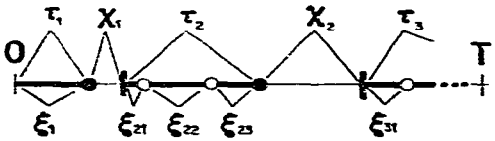

Fig. 1. Schematic representation of the fate of a protein molecule as a temporal sequence of collisions with and without interception. Intervals of motion of the molecule are drawn with heavy lines. Full circle, collision with interception; open circle, collision without interception; vertical bar, dissociation of the complex.

Using the language of stochastic processes, we can say that the fate of the protein molecule is a simple time-dependent process[4] with two states (rest and motion) and the transition intensities $\lambda = \omega\kappa$ and μ corresponding to transitions motion → rest and rest → motion, respectively. From the properties of the exponential distribution it follows that for the mean and variance of waiting times the following relationships hold (ref. 5, p. 8):

$$\left.\begin{aligned} \langle\tau_j\rangle &= \lambda^{-1} \quad ; \quad \operatorname{var}\tau_j = \lambda^{-2} \\ \langle\chi_j\rangle &= \mu^{-1} \quad ; \quad \operatorname{var}\chi_j = \mu^{-2} \end{aligned}\right\} \tag{3}$$

Hence, *e.g.*, λdt is the probability that a freely drifting molecule will suffer in the interval $t, t + dt$ an effective collision. The instants of state transitions of the molecule divide the interval of observation $[0, T]$ into a random number ν of subintervals of motion and rest of duration τ_j and χ_j, respectively ($j = 1, 2, \ldots$) (Fig. 1). Now, the main problem is to derive the distribution of the total time of motion τ within the interval $[0, T]$, *i.e.*, of the sum

$$\tau = \tau_1 + \ldots + \tau_\nu \quad ; \quad 0 \leqslant \tau \leqslant T \tag{4}$$

If the motion of the molecule were uniform with constant velocity v then its displacement s after time T would be simply a random variable, $s = v\tau$. However, as the motion is Brownian with drift, we have to take into consideration its property (ref. 5, p. 98; ref. 6, p. 274) that if the time of motion is $\tau = t$, then the displacement s_t is a normally distributed random variable with mean and variance being

$$\langle s_t\rangle = vt \quad ; \quad \operatorname{var} s_t = 2Dt \tag{5}$$

i.e. s_t will have the density

$$g(s|\,t) = \frac{1}{\sqrt{4\pi Dt}} \cdot e^{-(s-vt)^2/(4Dt)}$$

where v is the drift velocity and D the diffusion coefficient of the protein molecule in gel. However, in our model* the total time of mobility τ is a random variable capable of assuming any value from the interval $(0, T)$ with a probability density $f_T(t)$ (to be derived later). Hence the density of displacement s is obtained by summing all the densities $g(s|\,t)$ multiplied by the corresponding probabilities $f_T(t)$, namely

$$g(s) = \int_0^T f_T(t)\, g(s|\,t)\, dt \tag{6}$$

If many protein molecules start at time $t = 0$ and each of them independently executes this kind of random walk (a necessary condition for this is that their concentration is low enough to prevent mutual interaction), then the density function $g(s)$

* Using this simple model of diffusion we have obviously left out of consideration the existence of left and right barriers, *i.e.*, both ends of the gel rod, which in our case usually have only negligible effects.

yields the concentration profile of the protein zone for any given T. Exact calculation of the distribution of τ for arbitrary transition intensities λ and μ seems prohibitively cumbersome. For this reason we shall treat two special cases of importance:

(A) $\lambda = \mu$; this can be easily achieved experimentally by a suitable choice of ligand concentration c.

(B) $\lambda T \gg 1, \mu T \gg 1$, simultaneously. In other words, the mean waiting times $\langle \tau_j \rangle$ and $\langle \chi_j \rangle$, $j = 1, 2, \ldots$, are small in comparison with the time of observation T. This means that the fate of the protein molecule during time T will consist of many consecutive events of complex formation and its decay.

Before proceeding further, a note on the physical interpretation of the transition intensities λ and μ should be made. We have found above that $\lambda = \omega\kappa$, where ω is the effective cross-section of the complex formation reaction and κ is the collision intensity, *i.e.*, the mean number of collisions with ligands per unit time which a molecule suffers when drifting through the gel. The latter parameter is clearly linearly dependent on the ligand concentration c, at least within some reasonable range, and so also is λ. Therefore, following the custom in chemistry, we can write $\lambda = k_1 c$ because λ is in fact the rate of reaction $M + L \rightarrow ML$. Consequently, we have $\mu = k_2$, as this is the rate constant corresponding to reverse reaction $ML \rightarrow M + L$. Likewise, the association (equilibrium) constant is $K = k_1/k_2$.

(A) $\lambda = \mu$, *i.e.*, $k_1 c = k_2$. This case can be treated exactly and the derivation of the equations presented below is outlined in the Appendix (A). The probability density ϕ_m of the variable $x = \tau/T$, $0 < x \leqslant 1$, where τ is defined by eqn. 4 is given by the following expression, assuming that at $t = 0$ the protein molecule was free:

$$\phi_m(x) = \lambda T e^{-\lambda T} \cdot I_0[2\lambda T \sqrt{x(1-x)}] + \\ + \lambda T e^{-\lambda T} \sqrt{x/(1-x)} \cdot I_1[2\lambda T + \sqrt{x(1-x)}] + e^{-\lambda T} \delta(1-x) \quad (7)$$

where I_0 and I_1 are modified Bessel functions of order 0 and 1, respectively, defined by the expansion

$$I_\varrho(z) = \sum_{k=0}^{\infty} \frac{1}{k!\Gamma(k+\varrho+1)} \cdot \left(\frac{z}{2}\right)^{2k+\varrho} \quad (8)$$

(see ref. 5, p. 57, and ref. 7, p. 195) for $\varrho = 0$ and $\varrho = 1$ and δ is the Dirac function. The last term in eqn. 7 takes into account the case when the molecule happens to be still free at time $t = T$ without having suffered any effective collision. The required density of τ is obviously

$$f_{\tau,m}(t) = \frac{1}{T} \phi_m\left(\frac{t}{T}\right) \quad (9)$$

for $0 < t \leq T$ with the last term in eqn. 7 then reading $e^{-\lambda T} \cdot \delta_+(T - t)$. For small λT (λT is the mean number of state transitions during T), the density curve $\phi_m(x)$ is slightly asymmetric, as

$$\left\langle \frac{\tau}{T} \right\rangle = \frac{1}{2} + \frac{1}{4\lambda T}(1 - e^{-\lambda T})$$

With λT increasing, the second term on the right vanishes as well as the effect of discontinuity at $t = T$. Simultaneously, the variable τ tends asymptotically to normality so that we can consider τ as normally distributed with mean and variance

$$\langle\tau\rangle = \tfrac{1}{2}T, \qquad \text{var } \tau = T/(4\lambda) \tag{10}$$

The approximation of $f_{T,m}(t)$ by a Gaussian curve with $m = \frac{1}{2}T$ and $\sigma^2 = T/(4\lambda)$ is good enough even for moderate values of λT, as can be seen in Fig. 3.

So far we have assumed that at $t = 0$ the protein molecule is in a state of mobility (for that reason we used the subscript m in symbols ϕ_m and $f_{T,m}$). If the molecule is initially bound to a ligand, then the density corresponding to eqn. 7 is

$$\phi_b(x) = \lambda T e^{-\lambda T} \cdot I_0 [2\lambda T \sqrt{x(1-x)}] + \\ + \lambda T e^{-\lambda T} \sqrt{(1-x)/x} \cdot I_1 [2\lambda T + \sqrt{x(1-x)}] + e^{-\lambda T} \cdot \delta(0) \tag{11}$$

and

$$f_{T,b}(t) = \frac{1}{T} \cdot \phi_b\left(\frac{t}{T}\right) \tag{12}$$

corresponding to eqn. 8; the subscript b represents "bound". The distribution of the displacement s (the profile of the zone) is given by eqn. 6, where we insert 9 or 12 for $f_T(t)$ as the case may be. However, in practical applications we frequently find that diffusion is negligible compared with fluctuations arising from the intermittent random walk of the molecule. This will happen for small λT. In such a case the motion of the molecule can be considered as uniform with velocity v and the displacement is simply the variable $s = v\tau$. Then the corresponding density is

$$g(s) = \frac{1}{v} f_T\left(\frac{s}{v}\right) \tag{13}$$

If at $t = 0$ we start with a proportion γ of molecules in the state of mobility and $(1 - \gamma)$ molecules in the bound state $(0 < \gamma < 1)$, the profile of the zone will be given by

$$g(s) = \frac{1}{v}\left[\gamma f_{T,m}\left(\frac{s}{v}\right) + (1-\gamma) f_{T,b}\left(\frac{s}{v}\right)\right] \tag{14}$$

Especially if before switching on the voltage equilibrium is allowed to establish as determined by rate constants k_1 and k_2, we shall have

$$g(s) = \frac{Kc f_{T,m}\left(\frac{s}{v}\right) + f_{T,b}\left(\frac{s}{v}\right)}{(1 + Kc)\, v} \tag{15}$$

where $K = k_1/k_2$.

If diffusion cannot be neglected, then computation of functions 13, 14 and 15 requires numerical integration in accordance with eqn. 6.

(B) λT and μT both large. This case is described by the following approximate equations derived in the Appendix (B).

$$\langle\tau\rangle = \mu T/(\lambda + \mu) = T/(1 + Kc) \tag{16}$$

$$\text{var } \tau = 2\lambda\mu T/(\lambda + \mu)^3 = 2(Kc)^2 T/[k_1(1 + Kc)^3] = 2KcT/[k_2(1 + Kc)^3] \quad (17)$$

Taking into account the Brownian motion we obtain finally for displacement s

$$\langle s \rangle = v \langle \tau \rangle = v\mu T/(\lambda + \mu) = Tv/(1 + Kc) \quad (18)$$

$$\text{var } s = 2D \langle \tau \rangle + v^2 \text{ var } \tau = 2D\mu T/(\lambda + \mu) + 2\lambda\mu Tv^2/(\lambda + \mu)^3 = 2DT/(1 + Kc) + 2(Kcv)^2 T/[k_1(1 + Kc)^3] = 2DT/(1 + Kc) + 2KcTv^2/[k_2(1 + Kc)^3] \quad (19)$$

The term v^2 var τ represents the variance component resulting from the intermittent motion of the molecule. Excluding the extreme case of λ/μ either very large or very close to zero (cases of no practical interest in affinity electrophoresis; under such conditions either extremely high or extremely small retardation of the protein in affinity gel would be observed; in experiments aimed at evaluation of K the value of λ/μ should be approximately $1 < \lambda/\mu < 5$, the probability density of τ is unimodal and, within the limits of practically required accuracy, it may be approximated by normal density with mean m and variance σ^2 given by eqns. 16 and 17. Putting $\lambda = \mu$ we obtain the same $\langle \tau \rangle$ and var τ as given by eqn. 10. In case B it is irrelevant whether at time $t = 0$ the molecule is free or bound to a ligand. If diffusion is negligible, we can take s as approximately normally distributed with mean and variance

$$\langle s \rangle = v \langle \tau \rangle = Tv/(1 + Kc) \qquad \text{var } s = v^2 \text{ var } \tau = 2(Kcv)^2 T/[k_1(1 + Kc)^3]$$

as obviously derived from eqns. 16 and 17.

If, on the other hand, the diffusion is predominant with respect to fluctuations due to intermittent behaviour of the molecule, *i.e.*, if var $\tau \approx 0$, we can take s as approximately normal with mean and variance

$$\langle s \rangle = v \langle \tau \rangle = Tv/(1 + Kc) \qquad \text{var } s = 2D \langle \tau \rangle = 2DT/(1 + Kc)$$

RESULTS AND DISCUSSION

Effects of kinetics on the interacting protein zone profile: general exact solutions

One of the basic assumptions used so far in most studies employing affinity electrophoresis was that the kinetics of formation and dissociation of the protein–ligand complex can be considered very fast. This assumption implies that during the entire time of the electrophoretic experiment (T) each protein molecule enters many times into the complex, which again rapidly dissociates; in other words, the half-life $t_{1/2}$ of the complex is much shorter than T. Under such conditions the position of the centre of the zone of the interacting protein in the affinity gel bears a simple relationship to the concentration of the immobilized ligand and to the dissociation constant of the complex[2] and the width of the zone is determined essentially by diffusion. Because the protein spends a fraction of the total time in the non-diffusible complex, the diffusion broadening of the zone in an affinity gel is less than that in a control (non-interacting) gel, and characteristic "sharpening" of the interacting zones is observed. The degree of this sharpening (in relation to the control gel) is again

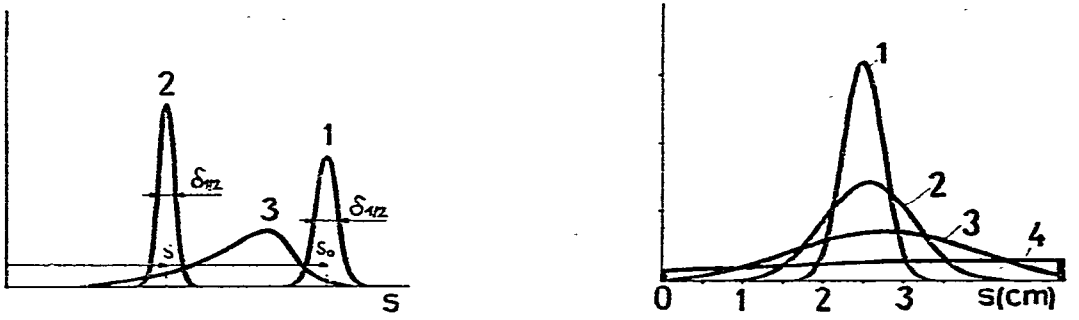

Fig. 2. Schematic comparison of the results of affinity electrophoresis in the case of very rapid kinetics and in the general case of slow kinetics. Abscissa, distance from the start; ordinate, protein concentration. Curve 1, concentration profile of the zone in control (non-interacting) gel. Curve 2, profile of the zone in an affinity gel in the case of very rapid kinetics. The width of the peak is determined predominantly by diffusion; it is less than the width of peak 1 because of the limited time spent in the free diffusable state. The value of s is given by $s/(s_0 - s) = 1/(Kc)$. Curve 3, as curve 2 but representing the general case of slow kinetics. Note that the exact determination of the position and width of the zone is difficult because of asymmetry and broadening caused by kinetic effects.

Fig. 3. Profiles of the zones of a ligand-binding protein in an affinity gel as calculated from eqns. 7 and 9. Abscissa, distance from the start; ordinate, protein concentration. In all cases the association (equilibrium) constant of the hypothetical complex is $K = 10^8$ l mol^{-1}, $c = 10^{-8}$ M, $T = 5000$ sec, $v = 10^{-3}$ cm sec^{-1}. The rate constants of complex dissociation were $k_2 = 2 \cdot 10^{-2}$, $4 \cdot 10^{-3}$, 10^{-3} and $2 \cdot 10^{-4}$ sec^{-1} for curves 1, 2, 3 and 4, respectively. These values correspond to 100, 20, 5 and 1 state transitions (free ↔ bound) of an average protein molecule during the entire time of the experiment. The half-width of the zone in the ideal case of very rapid kinetics ($k_2 \to \infty$) would be *ca.* 0.7 mm under otherwise identical conditions. The vertical heavy bar at the right-hand end of curve 4 denotes schematically the fraction of molecules migrating unretarded, *i.e.*, the molecules that did not suffer any productive collision with immobilized ligand during the entire time of the experiment. This fraction is negligibly small in the cases represented by curves 1–3.

simply related to the dissociation constant of the complex and concentration of the immobilized ligand[3].

In this study we have found quantitative relationships describing the effects expected in the case of non-negligible kinetic limitations of the complex formation and dissociation reactions. The essential result is that the kinetics of these reactions determine the width and generally the form of profile of the zone of the interacting protein in the affinity gel. This basic difference between the situation under the conditions of very rapid kinetics and in the case of slow kinetics is shown schematically in Fig. 2.

The general relationship applicable for the exact calculation of the profile of an interacting zone in the affinity gel is eqn. 6. As stated above, solution of this equation in the general case would be extremely difficult and therefore two simpler equations were derived that describe two special cases.

If $k_1 c = k_2$, *i.e.*, $Kc = 1$ (which can always be easily achieved by selecting an appropriate c; in the ideal case of very rapid kinetics this condition produces a 50% retardation of the protein in the affinity gel compared with the control gel, which is just optimal retardation for the determination of K), the zone profiles can be calculated exactly for any T using eqns. 7 and 9. The results obtained using eqn. 9 are shown in Figs. 3 and 4.

Fig. 3 demonstrates the dependence of the zone profile on the kinetic parame-

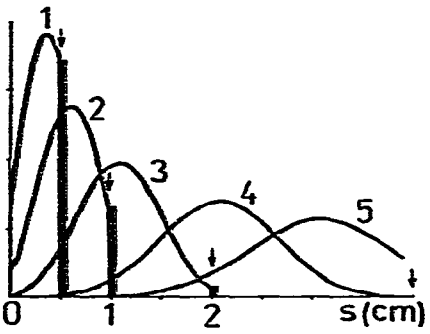

Fig. 4. Profile of the zone of a ligand-binding protein in an affinity gel for various observation times (*i.e.*, "development" of the profile during the experiment) as calculated from eqns. 7 and 9. Abscissa, distance from the start; ordinate, protein concentration. The hypothetical system is characterized by the following parameters: $k_1c = k_2 = \lambda = 3 \cdot 10^{-3}$ sec^{-1}, $v = 10^{-3}$ cm sec^{-1}. The observation times are $T = 500$, 1000, 2000, 4000 and 6000 sec for curves 1, 2, 3, 4 and 5, respectively. The arrows indicate the position of the centre of the zone in a control (non-interacting) gel for corresponding T. Vertical heavy bars at the right-hand ends of curves 1–3: see legend to Fig. 3 for explanation.

ters, namely on the lifetime of the protein–immobilized ligand complex at constant K, c, T and v. Clearly, the longer the lifetime of the complex (*i.e.*, the slower the dissociation reaction), the more "blurred" and asymmetric the zone is. Fig. 4 illustrates the development of the zone profile during electrophoresis; the increase in the zone width with time, the marked deviation of the position of the maximum from the "ideal" $s = \frac{1}{2}s_0$ value (which is observed in the case of rapid kinetics under otherwise identical conditions) and the asymmetry of the zone especially at the beginning of the experiment are obvious. It is clear that the magnitude of the effects predicted by eqn. 9 depends basically on the half-life of the complexes in relation to T and v; in principle, an appropriate decrease in v and increase in T should largely eliminate adverse effects of slow kinetics on the width of interacting zones. However, v and T can be varied in practice only in a limited range because of pronounced diffusion broadening of the zones at very large T.

Some typical examples

It is illustrative to consider examples of real protein–ligand systems and to guess whether they can be considered to undergo "rapid" or "slow" kinetics under typical conditions of affinity electrophoresis (Fig. 5). It is obvious that a typical lectin–sugar complex has a very short half-life and thus the kinetic effects occurring in affinity electrophoresis of such a lectin on an affinity gel containing immobilized sugar can be neglected and the results can be used for estimation of equilibrium constants in usual way (plotting $s/(s_0 - s)$ *vs.* $1/c$)*.

On the other hand, in cases of more stable high-affinity antibody–hapten complexes, the half-lives of the complexes are comparable to T, the zones are blurred and

* The values of the rate constants of the protein–ligand interactions[8,9] used in Fig. 5 must be taken only as rough approximations because they were obtained from studies in free solution; the rate constants of reactions with immobilized ligands may be different. We also neglect the effects of multiple sugar-binding sites in the lectin molecule; *i.e.*, we deal here with a hypothetical monovalent lectin.

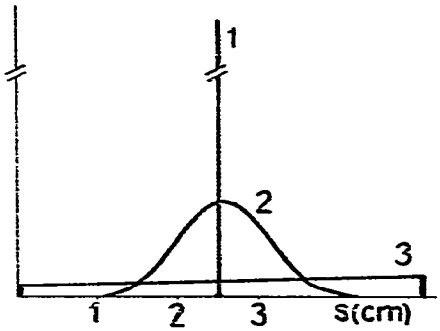

Fig. 5. Examples of the results of affinity electrophoresis expected for various ligand-binding proteins (based on eqns. 7 and 9). Curve 1, profile of the zone of a protein forming a complex characterized by $K = 10^4$ l mol^{-1} on a gel containing immobilized ligand ($c = 10^{-4}$ *M*); $k_1 = 10^5$ l mol^{-1} sec^{-1}, $k_2 = 1$ sec^{-1} (values corresponding approximately to those found for the interaction of a lectin with a carbohydrate ligand[8]). $T = 5000$ sec, $v = 10^{-3}$ cm sec^{-1}. Curve 2, as curve 1 but for a protein forming a complex characterized by $K = 10^{10}$ l mol^{-1} on a gel containing immobilized ligand ($c = 10^{-10}$ *M*); $k_1 = 4 \cdot 10^7$ l mol^{-1} sec^{-1}, $k_2 = 4 \cdot 10^{-3}$ sec^{-1}. Curve 3, as curve 2 but for a protein forming a more stable complex ($K = 2 \cdot 10^{11}$ l mol^{-1}, $k_1 = 4 \cdot 10^7$ l mol^{-1} sec^{-1}, $k_2 = 2 \cdot 10^{-4}$ sec^{-1}). In all cases $T = 5000$ sec, $r = 10^{-3}$ cm sec^{-1}. The proteins are assumed to be applied as an extremely narrow zone. The values characterizing curves 2 and 3 correspond approximately to the interaction of high-affinity antibodies with corresponding antigens or haptens[9].

estimation of s is difficult. A large increase in T (and a concomitant decrease in v) would be necessary to eliminate these adverse kinetic effects, which would be accompanied by unacceptable diffusion broadening of the zones.

Possibility of measurement of rate constants

These results have interesting experimental consequences as they suggest the possibility of estimating the kinetic parameters of protein–immobilized ligand complexation reactions. The rate constants should be determined from the zone profiles obtained under suitable conditions (c, v, T), at least for sufficiently slow reactions (*i.e.*, for relatively kinetically stable complexes with half-lives of approximately $t_{1/2} > 10$ sec). For less stable complexes the use of more sophisticated instrumentation (making possible, *e.g.*, work at very high potentials, thus producing high v, continuous scanning of the zone profile and very short observation times) would be necessary. Although this measurement of rate constants should be possible generally under the conditions assumed during the derivation of eqn. 9, experimentally it would be more convenient to work under the conditions described as case B, *i.e.*, eqns. 18 and 19, and to determine kinetic parameters from the half-widths of the symmetrical zones as discussed in the following section.

Use of simple approximate equations

Although eqns. 7 and 9 permit the exact calculation of the zone profiles, the solution requires numerical integration, preferably using a computer. However, as shown in Figs. 3 and 4, the zone profile can be approximated by a symmetrical Gaussian curve for moderate values of λT and eqns. 18 and 19 can be applied for calculation of $\langle s \rangle$ and zone width, respectively. Eqn. 19 is simple and easily applicable

to the rapid evaluation of kinetic effects on the zone width. The position of the maximum is identical with that expected in an ideal case of very rapid kinetics and eqn. 18 is identical with the original simple relationship used for calculation of apparent K as introduced originally by Gerbrandy and Doorgeest[10] and Takeo and Nakamura[11]. Eqn. 19 states that the zone width depends on two terms, the first being diffusion determined and the second kinetic dependent. The latter term decreases with increasing K, c, k_2 and k_1 and increases with time. It should be noted that eqns. 18 and 19 are approximate and their accuracy increases as λT increases. For practical purposes it is sufficiently exact for λT values higher than *ca.* 5 (Figs. 3 and 4). Under these conditions the results obtained by using eqns. 9 and 19 are almost identical. Eqns. 18 and 19 cannot be used for an adequate description of the initial phases of an electrophoretic experiment when λT is too low.

As stated above, eqn. 19 would be especially useful for the evaluation of the rate constants from the results of affinity electrophoresis. The following approach to a rough estimation of k_1 can be suggested. Let, e.g., the experimental conditions be such that eqns. 18 and 19 can be used; let s_0 denote the displacement of the molecule in a control gel and s the displacement in the affinity gel. If a value of c is used such as to yield $s = \frac{1}{2}s_0$ (*i.e.*, $Kc = 1$), then according to eqn. 19 we shall have

$$\text{var } s_0 = 2DT$$

$$\text{var } s = DT + v^2T/4\lambda$$

Assuming that v, c, T are known, k_1 is determined as follows:

$$\lambda = k_1c = v^2T/4(\text{var } s - \text{var } s_0)$$

where var s and var s_0 will be determined from the corresponding half-widths of the zones. Alternatively, a family of curves such as those in Figs. 3–5 can be generated on a computer and compared for best fit with that experimentally found.

Alternative approach: electrophoresis starts after establishment of equilibrium

The experimental design of all cases discussed so far was such that, at the beginning, the sample of protein molecules was on the upper surface of the gel rod and, after switching on the electric field, they migrated at a constant rate into the gel. Thus, at the beginning, all the protein molecules were in the free uncomplexed state and the steady state in the migrating zone was gradually established. However, a different approach is also possible, which is currently used in preparative affinity chromatography: the proteins are left to enter the affinity gel, the permeation is interrupted for a time sufficient for establishment of equilibrium and then permeation starts again. Analogously, in an electrophoretic system the sample would be electrophoresed into the uppermost part of the vertical gel (or applied on the surface of the horizontal gel), then the voltage would be switched off, equilibrium established and then electrophoresis continued. This case, *i.e.*, when initially a fraction of protein molecules is free and the remainder is bound in the complex (the proportion of the bound and free molecules is determined by the values of K and c) is described by eqn. 15. With complexes with relatively long lifetimes ($t_{1/2} > T$) an important result is to be expected from eqn. 15, as shown schematically in Fig. 6.

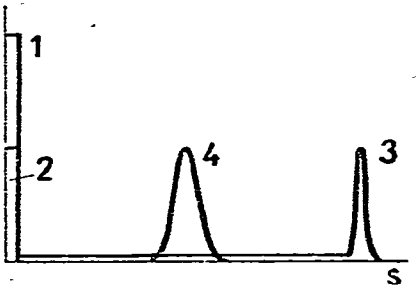

Fig. 6. Schematic representation of electrophoretic separation of complex-bound and free ligand-binding protein molecules for complexes of different stability as predicted by eqn. 15. Protein was allowed to enter the gel, the voltage was switched off and equilibrium was established (peak 1). After switching on the voltage, the free (uncomplexed) protein molecules (peak 3) migrate with velocity v; the rate of complex formation during their migration through the affinity gel is very low as the condition $k_1 c = k_2 \gg 1/T$ holds for very stable complexes. The fraction of protein molecules immobilized in the complex (peak 2) remains largely in its original position owing to very slow complex dissociation. Thus, the ratio of peak 2 to peak 3 can be used for calculation of K as it is very close to the bound/free ratio at equilibrium. In the case of a less stable complex ($k_2 < 1/T$) no separation of free and bound protein molecules occurs and a single zone is observed (peak 4).

As a result of slow complex decay, the separation of free and bound protein molecules will occur, two zones will be formed, and artificial "heterogeneity" will be observed. This phenomenon might be partly responsible for some instances of apparent glycoprotein heterogeneity as detected by affinity electrophoresis in agarose gels containing incorporated lectins[12,13], and it is also the basis of several variants of affinity electrophoresis employing separation of bound and free fractions of antibodies for the determination of equilibrium constants of their complexes with antigens[14,15].

It should be stressed again that this approach for determining dissociation constants is applicable only for complexes with very long lifetimes; for rapidly decaying complexes the results of affinity electrophoresis should be practically identical whether all protein molecules are initially free or the electrophoresis starts just after establishment of equilibrium.

Analogies with affinity chromatography and other techniques

It seems likely that kinetic limitations analogous to those examined in this study are the reason for pronounced broadening of the zones of ligand-binding proteins as observed in quantitative affinity chromatography[16,17]. The occurrence of this phenomenon in affinity chromatographic systems is at conspicuous variance with the results of affinity electrophoresis, where such broadening is usually not observed (at least in the relatively rapid reactions studied by this method so far). This difference is probably due to the major effects of an additional rate-limiting mechanism occurring in the chromatographic systems, *i.e.*, diffusion of the protein from the free liquid phase to gel beads and back.

Denizot and Delaage[18] analysed theoretically the effects of the kinetics of protein–immobilized ligand interactions based on the results of quantitative affinity chromatography. They also predicted zone broadening and asymmetry as a result of

relatively slow kinetics and the possibility of measuring rate constants from the results of quantitative affinity chromatography, and they also noted the complications caused by hydrodynamic peculiarities of the chromatographic systems.

The principle of affinity electrophoresis is very similar to that of electrophoresis in ion-exchange media[19–22]. In this method, the rate of movement of, *e.g.*, cations through a column of a cation-exchanger or cation-exchange paper in an electric field depends both on the ionic mobility and the affinity of the ion to the cation-exchange resin. It can be used, *e.g.*, for an efficient separation of inorganic ions[23]. The theory of this method has also been published[20]. Interestingly, zone spreading was observed experimentally in this technique and it was assumed to be primarily the result of inhomogeneities of the ion-exchange medium; the effects of the kinetics of the ion–matrix interaction were not considered[20].

CONCLUSION

The results of this study indicate that kinetic effects are of great importance for an adequate theoretical description and the practical applicability of affinity electrophoresis. We found that kinetic effects are negligible when affinity electrophoresis is used for the determination of dissociation constants of relatively short-lived protein–ligand complexes (approximately $t_{1/2} < 10$ sec under normally used experimental conditions), *i.e.*, in most practically encountered cases. We have also demonstrated the possibility of measuring rate constants by affinity electrophoresis, at least with relatively long-lived protein–ligand complexes. The simplicity of the systems used in this technique (in comparison with chromatographic systems) should be advantageous for its application in studies on the mechanisms of interaction of proteins or other biological macromolecules with immobilized ligands, including kinetic studies in such systems.

Our results are valid for the model of the interaction of a monovalent protein with an immobilized ligand. We have not dealt with more complicated cases of bi- or multivalent proteins or systems that contain, in addition to immobilized ligand, some mobile (free) ligand molecules. However, the approaches used and the results obtained should also be applicable as a basis for a theoretical description of more complicated models.

APPENDIX

Here we give an outline of the derivation of the equations presented in the earlier sections. In doing so we shall need some basic facts about the exponential distribution and those related to it, and these can most conveniently be found in standard books[5,6].

(A) $\lambda = \mu$

The process of state transitions in this instance is a Poisson process with transition intensity λ. Under the condition that the number of transitions in the interval of observation $(0, T)$ is n, $n > 0$, the transition instants $t_1, \ldots, t_n$ partition the interval $(0, T)$ into $n + 1$ disjoint subintervals of lengths $u_1 = t_1, \ldots, u_n = t_n - t_{n-1}, u_{n+1} = T - t_n$. The joint density of $u_1, \ldots, u_n$ is

$$g(u_1, \ldots, u_n) = n!/T^n \tag{20}$$

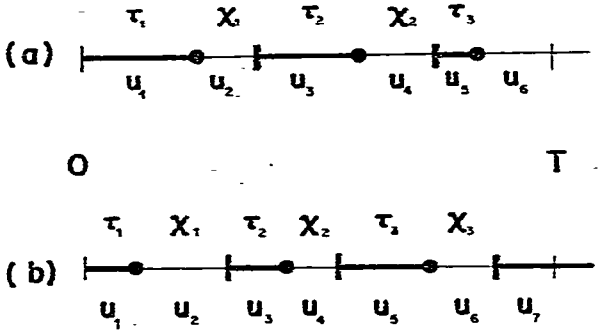

Fig. 7. Examples of partition of the interval of observation $[0, T]$ into subintervals of motion and rest by (a) an odd number ($n = 2k + 1 = 5$) and (b) an even number ($n = 2k = 6$) of transition occurrences assuming that at time $t = 0$ the molecule is free. Intervals of motion are drawn as heavy lines.

in the domain $0 < u_1 \leqslant \ldots \leqslant u_n < T$. The sum of the first r intervals $u_1 + \ldots + u_r$, $r \leqslant n$, has the density given by the beta distribution generalized to the interval $[0, T]$, *i.e.*,

$$b_{n,r} = \frac{n!}{(r-1)!(n-r)!}\left(\frac{t}{T}\right)^{r-1}\left(1 - \frac{t}{T}\right)^{n-r}\cdot\frac{1}{T} \tag{21}$$

(ref. 5, pp. 73–75; ref. 6, pp. 239–241). As the density 20 is invariant under any permutation of variables $u_1, \ldots, u_n$, the beta density $b_{n,r}$ holds for the sum of any selection of r variables out of $u_1, \ldots, u_n$. We shall use this fact in the sequel. Assuming that at $t = 0$ the molecule is free, we now wish to find the sum of all the subintervals of motion contained in $[0, T]$. We have to consider separately three cases according to whether the number of state transitions in $(0, T)$ is odd, even or zero.

(a) $n = 2k + 1$; $k = 1,2,\ldots$ From Fig. 7a (intervals of motion are drawn with heavy lines) we immediately see that the total duration of motion is

$$\tau = u_1 + u_3 + \ldots + u_{2k+1}$$

In accordance with what has been said above about the distribution of any selection of subintervals, it follows that τ has the density $b_{2k+1,\,k+1}(t)$.

(b) $n = 2k$; $k = 1,2,\ldots$ In this case the last interval of motion is the $(n + 1)$th interval which is cut off by instant $t = T$, as seen from Fig. 7b. However, we can use the same procedure as in case (a) by applying it to subintervals of rest. Evidently

$$\tau = T - (u_2 + u_4 + \ldots + u_{2k})$$

and as $u_2 + \ldots + u_{2k}$ has the density $b_{2k,k}(t)$, then τ has the density $b_{2k,k-1}(t)$ as follows from eqn. 21.

(c) $n = 0$. This means that the molecule drifted freely all the time T, so that simply $\tau = T$. Formally, the corresponding density is the Dirac function $\delta(t - T)$.

The densities of τ just found are conditional densities given a fixed number of state transitions in $(0, T)$. This number of transitions is a random variable, ν_T, obeying the Poisson law

$$Pr(v_T = n) = \frac{(\lambda T)^n}{n!} e^{-\lambda T}$$

Denoting by $f_{T,m}(t|\, n)$ the density of τ given $v = n$, the unconditional density of τ is obtained by randomizing the parameter n, *i.e.*,

$$f_{T,m}(t) = \sum_{n=0}^{\infty} Pr(v = n)\, f_T(t|\, n)$$

The right-hand side of this equation must, of course, be split into three terms with respect to cases (a), (b) and (c) as explained above. This means that we shall have

$$f_{T,m}(t) = \sum_{k=1}^{\infty} \frac{(\lambda T)^{2k+1}}{(2k+1)!} \cdot e^{-\lambda T} \cdot b_{2k+1,\,k+1}(t) + \sum_{k=1}^{\infty} \frac{(\lambda T)^{2k}}{(2k)!} \cdot e^{-\lambda T} \cdot b_{2k,\,k-1}(t) + e^{-\lambda T}\, \delta(t - T) \qquad (22)$$

Substituting explicit expressions for the beta densities in accordance with eqn. 21 and using the definition of the modified Bessel functions given by expansion 8, we arrive after some algebra at eqn. 7, if we change the variable τ to $x = t/T$.

The expectation of a variable with beta density 21 is $rT/(n + 1)$ (ref. 5, p. 49). The unconditional expectation $\langle\tau\rangle$ is then given by an expression analogous to the right-hand side of eqn. 22, if instead of the beta densities we insert the corresponding expectations.

The treatment of a molecule initially bound to a ligand proceeds along the same lines and need not be given here.

Now we have to derive an approximate equation for the density $\phi_m(x)$ expressed by eqn. 7 when λT is large. This we shall accomplish by investigating the asymptotic behaviour of a new variable

$$y = \sqrt{4\lambda T}\,(x - \tfrac{1}{2}) \quad ; \quad -\sqrt{\lambda T} \leqslant y \leqslant \sqrt{\lambda T} \qquad (23)$$

In order to save space and avoid clumsy equations we put $\lambda T = \alpha^2$, so that $y = 2\alpha(x - \frac{1}{2})$. The density of the variable y is then

$$\psi(y) = \frac{1}{2\alpha} \cdot \phi_m\left(\frac{y}{2\alpha} + \frac{1}{2}\right)$$

The corresponding explicit expression is obtained by substituting $x = \dfrac{y}{2\alpha} + \frac{1}{2}$ into $\phi_m(x)$. Thus we obtain

$$\psi(y) = \tfrac{1}{2}\,\alpha e^{-\alpha^2} \cdot I_0(z) + [(\alpha + y)/(\alpha - y)]^{\frac{1}{2}} \cdot \tfrac{1}{2}\alpha e^{-\alpha^2} \cdot I_1\, z \qquad (24)$$

where

$$z = \alpha^2 \left[1 - \left(\frac{y}{\alpha}\right)^2\right]^{\frac{1}{2}} = \alpha^2 - \tfrac{1}{2}y^2 - O(\alpha^{-2}) \qquad (25)$$

is the argument in the Bessel functions that occur in $\phi_m(x)$.

With y held fixed and α^2 increasing we can take advantage of the asymptotic formula for the Bessel function when z is large (ref. 7, p. 196):

$$I_\varrho(z) \sim e^z (2\pi z)^{-\frac{1}{2}}; \qquad \varrho = 0,1$$

Multiplying both sides of this asymptotic equivalence by $\frac{1}{2}\alpha e^{-\alpha^2}$, we obtain

$$\tfrac{1}{2}\alpha e^{-\alpha^2} I_\varrho(z) \sim \tfrac{1}{2}\alpha e^{-\alpha^2+z} \cdot (2\pi z)^{-\frac{1}{2}} \tag{26}$$

If now we put the expansion 24 of z into the right-hand side above and let $\alpha^2 \to \infty$, we find

$$\tfrac{1}{2}\alpha e^{-\alpha^2+z} \cdot (2\pi z)^{-\frac{1}{2}} \to \tfrac{1}{2} \cdot \frac{1}{\sqrt{2\pi}} \cdot e^{-\frac{1}{2}y^2} \tag{27}$$

As at the same time the factor $[(\alpha + y)/(\alpha - y)]^{\frac{1}{2}}$ in eqn. 24 tends to 1, we conclude from eqns. 24, 26 and 27 that

$$\psi(y) \sim \frac{1}{\sqrt{2\pi}} \cdot e^{-\frac{1}{2}y^2}$$

Consequently, the variable y is asymptotically normal with mean 0 and variance 1 for large values of $\alpha^2 = \lambda T$. Reverting to the original variable $\tau = xT$, it follows from eqn. 23 that

$$\tau = y\sqrt{\frac{T}{4\lambda}} + \frac{1}{2}T$$

Thus for large λT the variable τ is approximately normal with mean

$$\langle \tau \rangle = \tfrac{1}{2}T$$

and variance

$$\operatorname{var} \tau = T/4\lambda$$

or the corresponding standard deviation

$$\sigma = \sqrt{T/4\lambda}$$

With λT increasing the factor $e^{-\lambda T}$ in the Dirac functions in eqns. 7 and 11 tends to zero. Consequently, the normal approximation just found applies equally well to density $\phi_b(x)$, as is to be expected, as for large λT it is immaterial whether at time $t = 0$ the molecule was free or bound to a ligand.

(B) $\lambda \neq \mu$, both λT and μT large

We restrict our considerations to an approximate treatment of the problem by determining the mean and variance of the ratio

$$\eta = \sum_1^r \tau_j / (\sum_1^r \tau_j + \sum_1^r \chi_j) \quad ; \quad 0 < \eta \leqslant 1$$

when r is large. The variable η expresses the fraction of time the protein molecule spends in mobile state on condition that the number of disengagements from ligands, *i.e.*, of resumptions of its mobility after a state of rest, is equal to r. To remove the summation symbols we shall write hereafter $\tau(r) = \sum^r \tau_j$ and $\chi(r) = \sum^r \chi_j$ so that

$$\eta = \tau(r)/[\tau(r) + \chi(r)]$$

The two independent variables $\tau(r)$ and $\chi(r)$ have gamma distributions with parameters, r, λ and r, μ, respectively (ref. 5, p. 46), and their densities are not difficult to calculate. We refrain from doing so here and refer to Fig. 8 instead, where four examples of such a density are shown, namely for $\mu = 5\lambda$ and $r = 3$, 5, 10 and 20. Obviously, the distribution tends rapidly towards symmetry and its spread decreases. Hence we can use with confidence the following approximate equations for the mean and variance of η as a function of two uncorrelated variables $\tau(r)$, $\chi(r)$:

$$\langle \eta \rangle = \langle \tau(r) \rangle / (\langle \tau(r) \rangle + \langle \chi(r) \rangle) \tag{28}$$

$$\text{var } \eta = \left(\frac{\partial \eta}{\partial \tau(r)} \right)^2 \text{var } \tau(r) + \left(\frac{\partial \eta}{\partial \chi(r)} \right)^2 \text{var } \chi(r) \tag{29}$$

where both partial derivatives are to be understood at the respective points $\langle \tau(r) \rangle$ and $\langle \chi(r) \rangle$ (see ref. 23, Ch. 2, §14). From the properties of the gamma distribution (ref. 5, p. 46) it follows that $\langle \tau(r) \rangle = r/\lambda$, $\langle \chi(r) \rangle = r/\mu$, var $\tau(r) = r/\lambda^2$ and var $\chi(r) = r/\mu^2$. Executing the operations in eqns. 28 and 29 we find

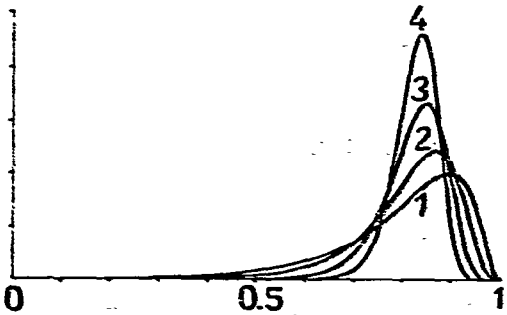

Fig. 8. Density of the ratio of total time of mobility to waiting time for the rth effective collision; curves 1, 2, 3 and 4 have been calculated for $r = 3$, 5, 10 and 20, respectively, and $5\lambda = \mu$. They exhibit a rapid approach to symmetry with increasing number of effective collisions.

$$\langle \eta \rangle = \mu/(\lambda + \mu)$$

$$\text{var } \eta = 2(\lambda\mu)^2/r(\lambda + \mu)^4 \tag{30}$$

Now the process of consecutive resumptions of mobility of the molecule is a renewal process with waiting times $\tau_j + \chi_j, j = 1,2,\ldots$, and the number r of such occurrences in the interval of observation $[0, T]$ is a random variable. According to the central limit theorem for renewal processes (ref. 5, p. 389), the number r for large λT, μT will be approximately normally distributed with expectation

$$\langle r \rangle = \lambda\mu T/(\lambda + \mu)$$

and variance

$$\text{var } r = \lambda\mu T\,(\lambda^2 + \mu^2)/(\lambda + \mu)^3$$

in consequence of eqns. 3. The standard deviation of r divided by $\langle r \rangle$ is inversely proportional to $\sqrt{\lambda T}$ and thus with increasing λT the relative variation of r diminishes. For large λT, μT we can put into eqn. 30 the mean $\langle r \rangle$ instead of r to obtain

$$\text{var } \eta \approx 2\lambda\mu/T(\lambda + \mu)^3$$

To derive the approximate expressions for the total time of mobility τ, we write $\tau = T\eta$, to obtain finally

$$\langle \tau \rangle \approx T\langle \eta \rangle = \mu T/(\lambda + \mu)$$

$$\text{var } \tau \approx T^2 \text{ var } \eta = 2\lambda\mu T/(\lambda + \mu)^3$$

For $\lambda = \mu$ we have $\langle \tau \rangle = \frac{1}{2}T$ and var $\tau = T/4\lambda$, in agreement with eqns. 10.

SYMBOLS

$\langle \ldots \rangle$	symbol for the mean value (expectation) of a random variable;
var...	variance of a random variable (second-order central moment often denoted by σ^2);
m	mean
σ	standard deviation } of normal (Gaussian) distribution;
$\delta_{1/2} = \sigma\sqrt{2 \ln 2}$	half-width }
ξ_j	waiting time between consecutive collisions;
χ_j	lifetime of a protein complex;
κ	collision intensity;
μ	intensity of complex decay;
ω	probability of interception by a ligand in a collision;
λ	interception intensity;
τ_j	time of uninterrupted motion of a molecule;

T	time of observation;
v	number of intervals of mobility within $[0, T]$;
$\tau = \sum_1^v \tau_j$	total time of mobility within $[0, T]$;
t	general variable for time;
s	displacement of the molecule, *i.e.*, distance travelled from the starting point during time T at potential gradient V;
v	drift velocity (m sec^{-1}) of electrophoretic motion in gel due to the field applied;
D	coefficient of diffusion (m^2 sec^{-1});
$f_{T,m}(t), f_{T,b}(t)$	density of total time of motion τ for molecule initially bound or free, respectively;
$\phi_m(x), \phi_b(x)$	density of the variable $x = \tau/T$; meaning of subscripts m and b as above;
$g(s)$	density of distance s; zone profile curve;
K	equilibrium (association) constant of the univalent protein ligand complex (l mol^{-1});
k_1	rate constant of the protein–immobilized ligand complex formation reaction (l mol^{-1} sec^{-1});
k_2	rate constant of complex decay reaction (sec^{-1});
$t_{1/2}$	half-life of a complex.

Units of transition intensities κ, μ and λ are sec^{-1} and of durations in sec.

ACKNOWLEDGEMENTS

We are indebted to Drs. M. Jílek, P. Klein and J. Turková for careful critical reading of the manuscript and to Dr. M. Lederer for drawing our attention to the technique of electromigration in ion-exchange resins.

REFERENCES

1 V. Hořejší, *Anal. Biochem.*, 112 (1981) 1–8.
2 V. Hořejší, *J. Chromatogr.*, 178 (1979) 1–13.
3 V. Hořejší and M. Tichá, *J. Chromatogr.*, 216 (1981) 43–62.
4 W. Feller, *An Introduction to Probability Theory and Its Applications*, Vol. I, Wiley, New York, London, Sydney, 2nd ed., 1957, p. 397.
5 W. Feller, *An Introduction to Probability Theory and Its Applications*, Vol. II, Wiley, New York, London, Sydney, 1966.
6 S. Karlin, *A First Course in Stochastic Processes*, Academic Press, New York, London, 1968.
7 H. B. Dwight, *Tables of Integrals and Other Mathematical Data*, Macmillan, New York, 1968.
8 R. M. Clegg, F. G. Loontiens and T. M. Jovin, *Biochemistry*, 16 (1977) 167–174.
9 R. B. Holzman and E. W. Voss, Jr., *Mol. Immunol.*, 18 (1981) 915–924.
10 Sj. J. Gerbrandy and A. Doorgeest, *Phytochemistry*, 11 (1972) 2403–2407.
11 K. Takeo and S. Nakamura, *Arch. Biochem. Biophys.*, 153 (1972) 1–7.
12 T. C. Bøg-Hansen, in J.-M. Egly (Editor), *Affinity Chromatography and Molecular Interactions*, Les Colloques de l'INSERM, INSERM, Paris, No. 86, 1979, pp. 399–416.
13 J.-P. Salier, L. Faye, D. Vergaine and J.-P. Martin, *Electrophoresis*, 1 (1980) 193–197.
14 M. Caron, A. Faure and P. Cornillot, *J. Chromatogr.*, 103 (1975) 160–165.
15 M. Caron, A. Faure, R. Keros and P. Cornillot, *Biochim. Biophys. Acta*, 491 (1977) 558–565.
16 B. M. Dunn and I. M. Chaiken, *Biochemistry*, 14 (1975) 2343–2349.

17 D. Eilat and I. M. Chaiken, *Biochemistry*, 18 (1979) 790–795.
18 F. C. Denizot and M. A. Delaage, *Proc. Nat. Acad. Sci. U.S.*, 72 (1975) 4840–4843.
19 K. S. Spiegler and C. D. Coryell, *Science*, 113 (1951) 546–547.
20 K. S. Spiegler and C. D. Coryell, *J. Phys. Chem.*, 56 (1952) 106–113.
21 G. Manecke, *Naturwissenschaften*, 39 (1952) 62–63.
22 G. Alberti, A. Conte, G. Grassini and M. Lederer, *J. Electroanal. Chem.*, 4 (1962) 301–308.
23 D. H. Menzel, *Fundamental Formulas of Physics*, Prentice-Hall, New York, 1955.